Impact of GOS and 2'-FL on the production and structural composition of membrane-associated exopolysaccharides by B. adolescentis and B. infantis

Ferrari, Michela; van Leeuwen, Sander S.; de Vos, Paul; Jurak, Edita; Walvoort, Marthe T. C.

Published in:
Carbohydrate Polymers

DOI:
10.1016/j.carbpol.2024.122660

Publication date:
2025

Carbohydrate Polymers 347 (2025) 122660

Contents lists available at ScienceDirect

Carbohydrate Polymers

journal homepage: www.elsevier.com/locate/carbpol

Impact of GOS and 2'-FL on the production and structural composition of membrane-associated exopolysaccharides by *B. adolescentis* and *B. infantis*

Michela Ferrari [a], Sander S. van Leeuwen [b,1], Paul de Vos [c], Edita Jurak [d], Marthe T.C. Walvoort [a,*]

[a] Stratingh Institute for Chemistry, University of Groningen, Nijenborgh 7, 9747 AG Groningen, the Netherlands
[b] Department of Laboratory Medicine, University of Groningen, University Medical Center Groningen, Groningen, the Netherlands
[c] Department of Pathology and Medical Biology, Immunoendocrinology, University of Groningen, University Medical Center Groningen, Groningen, the Netherlands
[d] Department of Bioproduct Engineering, Engineering and Technology Institute Groningen, University of Groningen, Groningen, the Netherlands

ARTICLE INFO

Keywords:
Exopolysaccharides
Bifidobacteria
2′-fucosyllactose
Galactooligosaccharides
NMR spectroscopy
HPAEC analysis

ABSTRACT

Bifidobacteria, which are increasingly linked to health benefits to the host, produce structurally complex exopolysaccharides which are considered to be effector molecules responsible for health effects. It is currently not clear how the bacterial growth conditions, and especially the carbon source, affect the structural composition of the EPS. Here we present our investigations into the impact of the addition of 2′-fucosyllactose (2'-FL) and galactooligosaccharides (GOS), which are non-digestible carbohydrates added to infant formula, as the sole carbon source during the growth of *B. adolescentis* and *B. infantis*. Intriguingly, *B. adolescentis* produced EPS with larger molecular weights in the presence of GOS or a mixture of GOS/2'-FL. *B. infantis* showed increased growth levels in the presence of 2'-FL, and also produced an α-1,4-glucan polymer, whose amount was increased when grown on GOS. These findings highlight the species-specific effects of growth conditions on EPS structures.

1. Introduction

Exopolysaccharides (EPS) from probiotic bacteria receive increasing attention as one of the actors of the health effects associated with probiotic bacteria, with a focus on EPS from lactobacilli and bifidobacteria (Abdalla et al., 2021; Hidalgo-Cantabrana et al., 2014; Yang et al., 2023). Although their production and isolation are more challenging than EPS from lactobacilli, several bifidobacterial EPS structures have been isolated and characterized (Pyclik et al., 2020). However, a clear understanding of the EPS structures that confer a health benefit is lacking, mainly due to the low yields and the fact that EPS isolates are often present as heterogeneous mixtures. Increasing EPS yields and tuning the EPS structure might therefore be strategies to strengthen and shape the biological effects of these complex carbohydrates.

It is recognized that one of the factors that can influence bacterial growth and EPS production is the carbon source present in the growth media (Torino et al., 2015). When *Oenococcus oeni* was grown on either glucose or fructose, or a mixture of the two, it was found that the strain growth and ability to produce EPS was highly impacted by the carbon source. Fructose stimulated the growth of the strain the most, and the combination of the two carbohydrates resulted in higher EPS yields (Ibarburu et al., 2007). These results were attributed to the fact that fructose can both act as a fermentable substrate and as an electron acceptor, which can produce $NAD(P)^+$ after being reduced to mannitol. The cofactor can then be utilized both for bacterial growth and EPS biosynthesis.

Interestingly, the monosaccharide content of EPS seems also to be impacted by the carbon source (De Vuyst & Degeest, 1999; Looijesteijn et al., 2001). When grown in the presence of lactose or glucose, *Lactobacillus delbrueckii* subsp. *bulgaricus* NCFB 2772 produced higher EPS amounts compared to when grown in the presence of fructose (at equal cell density). In addition, the carbohydrate source also had an impact on the EPS composition: when the strain was grown on lactose, the resulting EPS was composed of galactose/glucose/rhamnose with a ratio of 6.8/1.0/0.7, whereas fructose had a negative impact on EPS yield (32 mg/L with lactose versus 8 mg/L with fructose) (Grobben et al., 1995) and led to an EPS composed of galactose/glucose in a ratio of 2.5/1.0 (De Vuyst & Degeest, 1999). Also for *Lactobacillus casei* it was found that

* Corresponding author at: Nijenborgh 7, 9747 AG Groningen, the Netherlands.
E-mail addresses: m.ferrari@rug.nl (M. Ferrari), sander.vanleeuwen@hvhl.nl (S.S. van Leeuwen), p.de.vos@umcg.nl (P. de Vos), e.jurak@rug.nl (E. Jurak), m.t.c.walvoort@rug.nl (M.T.C. Walvoort).
[1] Present address: Van Hall Larenstein, University of Applied Science, Department Forensic Laboratory Science, Leeuwarden, The Netherlands)

https://doi.org/10.1016/j.carbpol.2024.122660
Received 23 May 2024; Received in revised form 23 August 2024; Accepted 24 August 2024
Available online 26 August 2024

the EPS monosaccharide composition is influenced by the carbon source, with higher amounts of glucose detected when the strain was grown in the presence of milk supplemented with sucrose or glucose (Looijesteijn et al., 2001). Similarly, *Lactobacillus rhamnosus* EPS structure was found to be differently impacted by the presence of five different carbon sources (Polak-Berecka et al., 2013).

Although the exact mechanism through which the carbohydrate carbon source impacts the EPS biosynthesis is currently not known, gene expression studies may shed some light on this process. When the effect of different carbon sources on gene expression levels in *Bifidobacterium longum* subsp. *longum* CRC002 was investigated, a complex scenario was revealed in which different carbohydrates tune the transcription of genes involved in EPS biosynthesis, but also the stage of bacterial growth influences this process (Polak-Berecka et al., 2013). In addition, for *Lactobacillus paracasei* a specific mixture of carbon sources was found to positively influence EPS yield and monosaccharide composition, presumably by modulating the enzymatic activity in the EPS synthetic pathways (Yu Zhang et al., 2021).

Nutrition plays an important role in early life as it guides the colonization of the gut microbiota and contributes to the maturation of the gut mucosal immune system (Kong et al., 2020). Nowadays, non-digestible carbohydrates (NDCs) are added to infant nutrition to mimic some functions of human milk oligosaccharides (HMOs), including their prebiotic properties and their immune regulating effects (Bode, 2012; Cheng et al., 2021). Galactooligosaccharides (GOS) and 2′-fucosyllactose (2'-FL) (Fig. 1) are commonly added to infant formula (Garrido et al., 2013; Zeuner et al., 2019) due to their immune-stimulating and prebiotic properties. Their use has been associated with an increased colonization of the infant gut by bifidobacteria, which are linked to a healthy microbiota (Martins et al., 2019; Vandenplas et al., 2018). Interestingly, little is known about the effect of GOS and 2'-FL on bifidobacterial EPS production and structural composition.

Based on our hypothesis that GOS and 2'-FL can impact the yield and composition of the EPS produced by bifidobacteria, we present here our study into the effects of GOS and 2'-FL on the growth and EPS production by *Bifidobacterium adolescentis* and *Bifidobacterium longum* subsp. *infantis* (*B. infantis*). The EPS structures were investigated by the combination of High-Performance Anion Exchange Chromatography with Pulsed Amperometric Detection (HPAEC-PAD), Ultra-high Performance Liquid Chromatography with Fluorescence Detection (UPLC-FLD), Gel Permeation Chromatography (GPC) and one- and two-dimensional proton and carbon Nuclear Magnetic Resonance (1D/2D $^{1}H/^{13}C$ NMR) spectroscopy analysis, which allowed the determination of putative repeating units for the EPS produced by the two strains. Our study provides insight into how GOS and 2'-FL as the carbon source might modulate the EPS of *Bifidobacterium adolescentis* and *Bifidobacterium infantis* in the intestine of infants. In addition, these carbon sources could be a valuable mean to tune the structure of these surface carbohydrates and, consequently, their potential biological activity.

2. Materials and methods

2.1. Bacterial cultures

B. adolescentis DSM20083 and *B. longum* subsp. *infantis* DSM20088 were purchased from the German Collection of Microorgansims and Cultures DSMZ (Braunschweig, Germany). Peptone (catalog number 91249) and beef extract (catalog number B4888) were purchased from Sigma Aldrich (St. Louis, USA). 2'-FL (batch 105VXKD) and Vivinal GOS (batch BB11XTW) were provided by FrieslandCampina (Amersfoort, The Netherlands). The purity of the 2'-FL and GOS samples was determined with HPAEC-PAD (Table S1).

Bacteria were grown in MRS4 medium (Table S2), which contains glucose as the carbon source. For the GOS and 2'-FL-supplemented media, glucose was replaced by GOS and 2'-FL respectively. In the case of the GOS/2'-FL medium the ratio of GOS and 2'-FL was 4/1. Anaerobic conditions for liquid cultures were achieved by Hungate technique (Macy et al., 1972). Briefly, Hungate tubes and bottles containing liquid cultures were flushed with CO_2 to create anaerobic condition. For growth studies, the OD_{600} was measured sampling from 5 mL liquid cultures. For EPS isolation, the strains were inoculated in 5 mL medium and then sub-cultured in 300 mL of fresh medium and incubated anaerobically at 37 °C till OD_{600} reached 2.5–3.1.

2.2. Isolation procedure of membrane-associated EPS

EPS was isolated as previously described (Ferrari et al., 2022). Briefly, cells were harvested from 300 mL liquid cultures by centrifugation (7000 rpm, 5 °C, 15 min), washed once with PBS buffer (pH 7.5) and treated with 20 mL of 2 M NaOH and shaken overnight at room temperature. The cellular suspension was centrifuged (7000 rpm, 5 °C, 30 min) and two volumes of EtOH were added to the supernatant to precipitate the polysaccharides at −20 °C. After centrifugation (7000 rpm, 5 °C, 30 min) the pellets were resuspended in MilliQ water and dialyzed (3.5 KDa MWCO) against 2 L of MilliQ water at 4 °C for 48 h. The solution was lyophilized to obtain crude EPS.

2.3. Monosaccharide composition and quantification by HPAEC-PAD

EPS were hydrolyzed using an adapted method based on a previously described procedure (Jurak et al., 2014). In brief, samples (~5 mg) were treated with 0.45 mL 72 % H_2SO_4 (1 h, 30 °C) and then hydrolyzed with 2.8 M H_2SO_4 for 3 h at 100 °C. Samples were diluted (35×) and 10 μL were directly injected for analysis. High performance anion exchange chromatography (HPAEC) was performed on a Dionex Ultimate 6000 system (Thermo Scientific, Sunnyvale, CA, USA) equipped with a CarboPac PA-1 column (2 mm × 250 mm ID) in combination with a CarboPac PA-1 guard column (2 mm × 50 mm ID) and pulsed amperometric detection (PAD). The system was controlled by Chromeleon 7.2.9 software (Thermo Scientific, Sunnyvale, CA, USA). Elution of monosaccharides was performed at a flow-rate of 0.25 mL/min with a multi-step-gradient using the following eluents: A: 0.1 M NaOH, B: 1 M NaOAc in 0.1 M NaOH, C: 0.2 M NaOH, and D: MilliQ water. The gradient used was 16 % A, 84 % D (20 min), 45 % A, 5 % B, 50 % D (5 min), and 60 %

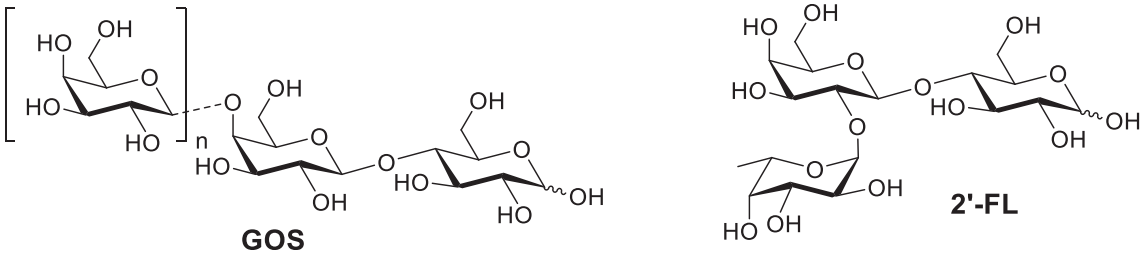

Fig. 1. Oligosaccharides used in this study as carbon source for the growth of *B. adolescentis* and *B. longum* subsp. *infantis*.

A, 40 % B (15 min). To regenerate the column, it was flushed during 12 min with 100 % C by increasing the flow-rate in the first 2 min to 0.35 mL/min. Finally, the column was equilibrated for 12 min with 16 % A, 84 % D by decreasing the flow-rate in the first 2 min to 0.25 mL/min. Pure monosaccharides (Sigma-Aldrich) were used as standards for quantification, and were dissolved in MilliQ water prior to analysis.

2.4. Monosaccharide composition analysis by UPLC-FLD

From a 10 mg/mL EPS stock solution a working solution (~1 μg/mL) was prepared in MilliQ water and 20 μL of the working solution were dried under a N_2 flow in 0.5 mL Eppendorf tubes. 10 μL of xylose (0.1 nmol/μL) were added as internal standard. A calibration curve was generated for GalNAc, GlcNAc, Gal, Man, Glc, Fuc (0.8–0.005 nmol/μL). All samples, including the standards, were hydrolyzed with 20 μL 2 M TFA (3 h, 90 °C). After drying under N_2, the samples were reconstituted in 10 μL NaOAc (80 mg/mL) and labeled with 20 μL 2-AA (30 mg/mL anthranilic acid and 30 mg/mL $NaCNBH_3$ in 2 % boric acid/methanol) for 1 h at 80 °C. The reaction was stopped by adding 250 μL Milli-Q water and separated on a Waters Acquity H-class UPLC system with FLD detector. The gradient consisted of A: 9 % ACN, 2 % triethylamine; 3 % H_3PO_4 in H_2O, and B: 50 % Buffer A in 50 % ACN. Separation was performed on a C18 column (2.1 × 50 mm) eluted with a gradient of 7 % A – 26 % A over 10 min at 0.19 mL/min, followed by a wash phase and reconstitution using 100 % A, followed by 7 % A.

2.5. Sialic acid analysis

Duplicate samples of *B. adolescentis* (GOS/2'-FL) EPS ~10 μg were hydrolysed using 2 M acetic acid at 65 °C for 2 h. After drying under N_2, the samples were labeled with 10 μL DMB (0.7 mg/mL 4,5-methylenedioxy-1,2-phenylenediamine dihydrochloride and 3 mg/mL sodiumhydrosulfite in 30 % acetic acid/methanol containing 2-mercaptoethanol) for 2 h at 50 °C. Samples were diluted with 150 μL MilliQ water and separated using a Waters Acquity H-class UPLC system with fluorescence detector. Separations were performed on a C18 column (2.1 × 50 mm Waters BEH), eluted under isocratic conditions with 10 % acetonitrile and 5 % methanol in water at 0.23 mL/min. A panel of reference sialic acids were treated similarly for elution time reference; i.e. Neu5Ac, Neu5Gc, Kdo and Kdn.

2.6. Molecular weight determination

The molecular weight of the samples was measured by gel permeation chromatography (GPC). The analysis was performed on an Agilent Technologies 1200 Series using three PSS Suprema columns (100, 1000, 3000 Å, 300 × 8 mm × 10 μm), with 40 °C column temperature. The eluate was monitored by a refractive index (RI) detector. The mobile phase was 0.05 M $NaNO_3$ at a flow rate of 1 mL/min. The sample concentration was 2 mg/mL and the injection volume was 10 μL. Ethylene glycol 0.5 % was used as internal standard. Calibration was performed using a pullulan series (PSS-pulkit-12, Polymer Standard Service) with a molecular weight in the range of 1.03–708 kDa.

2.7. Determination of protein content

The protein content of the samples was determined by the Bradford assay, using the Bio-Rad assay reagents (catalog number 500–0116); bovine serum albumin (BSA) was used to generate a standard curve. Absorbance was measured at 750 nm with a BioTek Synergy H1 plate reader.

2.8. Hygroscopicity test

The water content of three test-EPS samples was measured by weighing the samples before and after incubation at 60 °C for 7 days.

2.9. NMR spectroscopy

^1H and ^{13}C NMR spectra were recorded on a Bruker Avance NEO (600/150 MHz). Chemical shifts are given in ppm with the solvent resonance as internal standard (acetone: δ 2.225 ppm, or HDO: δ 4.79 ppm for ^1H). Samples were dissolved in 500 μL D_2O and lyophilized (2×) before performing NMR analysis. All individual signals were assigned using 2D NMR spectroscopy: 2D ^1H—^1H COSY, TOCSY (30, 60, 120 and 180 ms mixing times), ROESY (300 ms mixing time) and NOESY (200 ms mixing time) spectra were recorded using WET1D water suppression. Spectra were recorded with 2000–4000 complex points in t1 and 200–400 increments in t2, recording 8–32 scans, depending on sample quantity and experiment type. Two-dimensional ^{13}C—^1H correlation spectra, HSQC with multiplicity editing and HMBC with single bond suppression were recorded using 16–64 scans per increment, recording 2000 complex points and 200 increments.

3. Results

3.1. Bacterial growth in the presence of 2'-FL and GOS

First, the ability of *B. infantis* and *B. adolescentis* to grow in the presence of GOS, 2'-FL and a combination of the two oligosaccharides (ratio GOS/2'-FL, 4/1) as the sole carbon source, was investigated. The growth medium was based on the previously developed MRS4 medium, which was found to sustain excellent growth for both strains, while it lacks yeast extract that may interfere with EPS isolation (Ferrari et al., 2022). The exact composition of the MRS4 medium, which was used as a positive control for growth, and of the media with 2'-FL and GOS as the carbon sources can be found in Table S2.

As shown in Fig. 2, the growth of both *B. adolescentis* and *B. infantis* in the presence of GOS and GOS/2'-FL was comparable to the control (glucose), with *B. adolescentis* in GOS and *B. infantis* in GOS/2'-FL reaching a slightly higher OD_{600} after 24 h incubation than the other cultures. Interestingly, the culture of *B. infantis* in the presence of 2'-FL reached a very high density of ~2.3 after 24 h, whereas *B. adolescentis* was unable to grow in the presence of 2'-FL, in accordance with previous observations (Salli et al., 2021).

3.2. EPS isolation

Having established that the two strains were able to grow in the presence of the selected oligosaccharides, with the exception for *B. adolescentis* in 2'-FL, the EPS were isolated from *B. infantis* and *B. adolescentis* after growth in the presence of the different carbon sources (the 2'-FL- containing medium was not used for *B. adolescentis* due to the lack of growth). Because both OD_{600} and growth time can have an impact on the EPS isolate,(Petry et al., 2000) it was decided to grow all liquid cultures to an optical density of approximately 3.0, which was reached after different growth times (Table 1).

As shown in Table 1, *B. adolescentis* produced similar amounts (16–28 mg from 300 mL cultures) of EPS in all of the three media screened, with the glucose-containing MRS4 medium as the most effective for EPS production, and the GOS supplementation leading to the lowest EPS yield. In contrast, *B. infantis* showed overall higher yields of EPS (57–87 mg from 300 mL cultures) than *B. adolescentis*, in line with previous observations,(Ferrari et al., 2022) with GOS as the carbon source that stimulated the higher amount of EPS in the strain. Interestingly, when 2'-FL was used in combination with GOS, the EPS yield dropped to a value comparable to the one obtained with only 2'-FL. This result highlights the intriguing interplay of enzymes that are involved in uptake and fermentation of different carbohydrates. It was previously observed that GOS fermentation by infant fecal microbiota is preferred over 2'-FL fermentation, when supplied simultaneously (Akkerman et al., 2022). At the same time 2'-FL fermentation seems to be kick-started in the presence of GOS. Another explanation for this result

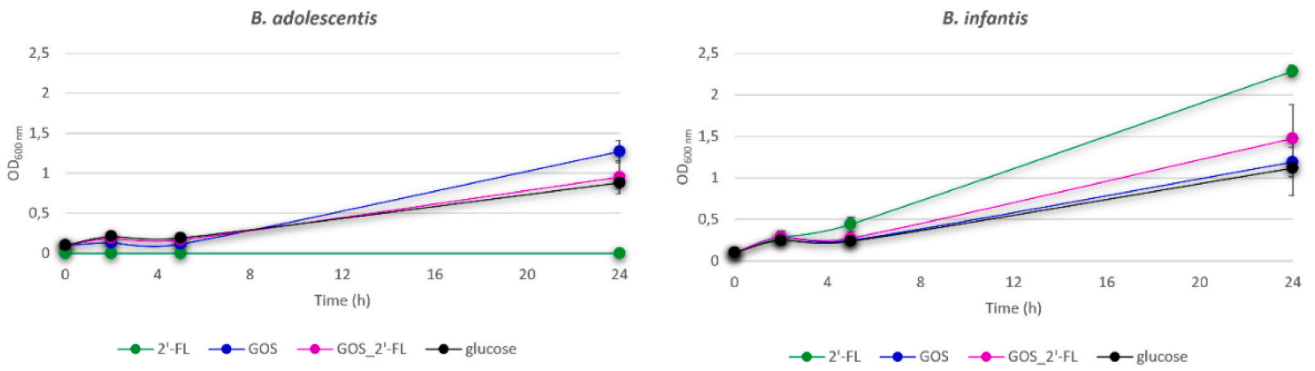

Fig. 2. Growth of *B. adolescentis* and *B. infantis* in medium containing 2'-FL (green), GOS (blue), GOS/2'-FL 4/1 (pink) and glucose (MRS4, black) measured in OD_{600}. The OD_{600} values are mean values ± SD ($n = 3$).

Table 1
Yields of isolated EPS, OD_{600} and growth times of the 300 mL liquid cultures. The values are mean ± SD ($n = 3$). [a] n.d. = not determined, as no growth was observed of *B. adolescentis* with 2'-FL as the sole carbon source; [b] GOS/2'-FL ratio of 4/1 (*w*/w); [c] Glc = glucose.

Strain	Carbon source	OD_{600}	Growth time (h)	Isolated material (mg/300 mL)
B. adolescentis	2'-FL	n.d. [a]	n.d. [a]	n.d.[a]
	GOS	2.8–3.1	72	16 ± 3
	GOS/2'-FL[b]	2.7–3.0	48	26 ± 6
	Glc[c]	2.7–3.0	72	28 ± 2
B. infantis	2'-FL	3.0–3.2	72	53 ± 5
	GOS	2.5–3.0	48	87 ± 7
	GOS/2'-FL[b]	2.9–3.2	48	57 ± 2
	Glc	2.7–3.1	48	65 ± 4

may be found in the expression levels of transport machinery. GOS and 2'-FL both have dedicated cellular transporters in *B. infantis* (ABC transporters (Garrido et al., 2013) and fucosyllactose transporters similar to ABC transporters,(Ojima et al., 2022) respectively), and previous findings suggested that 2'-FL addition leads to the upregulation of a large variety of transport system genes in *B. infantis* Bi-26,(Zabel et al., 2019) possibly resulting in preferential digestion of fucosylated glycans. In addition, the first step in 2'-FL degradation is performed by a fucosidase enzyme that removes the L-fucose residue, followed by further fermentation by galactosidase enzymes that also degrade GOS molecules (Bunesova et al., 2016). The carbon source may also differently impact the expression levels of these glycosyl hydrolases.

3.3. Chemical composition of the EPS samples

To determine the monosaccharide composition of the EPS isolations, acidic hydrolysis using TFA was performed followed by UPLC-FLD analysis, because sulfuric acid hydrolysis provided low carbohydrate content values (vide infra). As shown in Table 2, the EPS of both strains are composed of glucose and galactose, albeit in different ratios. For the different EPS samples from *B. adolescentis* only minor variations in the monosaccharide composition were detected between EPS from different growth conditions. This finding suggests that the carbon source had little impact on the EPS structure of *B. adolescentis*. In contrast, for *B. infantis* marked differences were observed in the monosaccharide ratios of EPS when growing bacteria with different carbon sources. As shown in Table 2, the presence of 2'-FL and GOS/2'-FL resulted in a decreased glucose/galactose ratio. Specifically, the EPS samples obtained from the GOS- and glucose-containing media both show a monosaccharide ratio with a slight excess of glucose (Glc: Gal ratios of 1.5: 1 for both), whereas the EPS samples isolated from media containing 2'-FL and GOS/2'-FL show a higher amount of galactose, compared to glucose (Glc: Gal ratios of 1: 1.6 and 1: 2.3, respectively). These results suggest that GOS and glucose have a similar effect on EPS structure and composition, whereas the presence of 2'-FL results in a different EPS structure.

Table 2
Monosaccharide composition and carbohydrate content of the EPS isolated from media containing different carbon sources following mild TFA hydrolysis and analysis using UPLC-FLD. The values are mean ± SD ($n = 3$). [a] Values were obtained using HPAEC-PAD analysis after sulfuric acid hydrolysis.

	Carbon source	Glc: Gal ratio	Carbohydrate content (w/w%)
B. adolescentis	GOS	2.5: 1 (± 0.2)[a]	19 ± 7[a]
	GOS/2'-FL	3.2: 1 (± 0.11)	17.2 ± 1.8
	Glucose	3: 1 (± 0.3)[a]	18 ± 11[a]
B. infantis	2'-FL	1: 1.6 (± 0.04)	73.7 ± 1.8
	GOS	1.5: 1 (± 0.04)	76.2 ± 6.8
	GOS/2'-FL	1: 2.3 (± 0.03)	52.5 ± 0.2
	Glucose	1.5: 1 (± 0.04)	72.5 ± 2.9

The carbohydrate and protein content of the EPS samples was investigated to assess purity. Initially, the samples were hydrolyzed using sulfuric acid and monosaccharides were quantified by HPAEC-PAD analysis (Table S3), as described previously (Ferrari et al., 2022). However, using this method unusually low carbohydrate content values were obtained. In the case of *B. adolescentis* the extended growth times (48 h and 72 h) might have caused the drop in carbohydrate content since the growth phase has a known impact on EPS production (Teixeira, 2014). However, the same reasoning cannot explain the deviation reported in the *B. infantis* samples, where the growth time was kept consistent (48 h) with the previous work (Ferrari et al., 2022). As the presence of water in the samples may cause an underestimation of the concentration of the samples used for the HPAEC-PAD analysis, three samples were subjected to a hygroscopicity experiment. After incubation at 60 °C for 7 days, the mass reduction was evaluated, and for two samples it was estimated to be around 20 % and 30 % (Table S4). This experiment shows that the carbohydrate content of EPS samples may be subject to variations as a consequence of their hygroscopic character. Following the low carbohydrate content values, it was decided to investigate if the acidic hydrolysis method employed for the samples could have impacted the carbohydrate content due to monosaccharide degradation (Harazono et al., 2011; Shi et al., 2012). The samples (*B. adolescentis* GOS/2'-FL and *B. infantis* 2'-FL, GOS/2'-FL, GOS and glucose) were treated with 2 M TFA at 90 °C for 3 h and the carbohydrate content was measured by UPLC-FLD analysis (Table 2). It was found that the carbohydrate content of *B. infantis* 2'-FL, GOS and glucose increased from ~30 % to ~70 % and the carbohydrate content of *B. infantis* GOS/2'-FL increased from ~18 % to ~53 %. These results suggest that the treatment with H_2SO_4 might have contributed to the low recovery observed for these samples. On the other hand, the carbohydrate content for *B. adolescentis* GOS/2'-FL did not increase when the milder TFA hydrolysis protocol was used (Table 2, Table S3).

However, the carbohydrate content measured here did not include the contribution of sialic acid, which was identified using NMR spectroscopy and UPLC-FLD after DMB labeling, as presented in section 3.4.1 (vide infra). The protein content of all samples was assessed by the Bradford assay. All values ranged below 8 % *w*/w showing a minor protein contamination (Table S3).

To assess the impact of the carbon source on the molecular weight distribution of the EPS samples, the size distribution profile was analyzed by gel permeation chromatography (GPC). As shown in Fig. 3 (panel A), *B. adolescentis* consistently produced one polymeric population composed of polysaccharides with higher molecular weights in the presence of GOS and GOS/2'-FL than those obtained from cultures with glucose. On the other hand, three polymeric populations are visible in the *B. infantis* samples (Fig. 3, Panel B). All samples contain a similar population of smaller polysaccharides (~ 10 kDa), whereas larger variation is observed in the high MW populations. The EPS samples from *B. infantis* in 2'-FL and in GOS/2'FL contain one population with 100–300 kDa MW range. Interestingly, the EPS samples from *B. infantis* in GOS and glucose contain an additional high-molecular weight population with highest MW range (334–708 kDa). Taken together, these results suggest that GOS in *B. adolescentis* impacts gene expression of genes involved in polysaccharide chain-length determination, an effect that is absent when grown with glucose. For *B. infantis*, it seems that the presence of GOS and glucose impacts the chain elongation machinery, or possibly the production of other EPS types.

3.4. Structural characterization of the EPS samples using NMR

3.4.1. EPS samples from B. adolescentis

As described in the previous section, HPAEC and UPLC analysis suggested that *B. adolescentis* EPS samples are composed of glucose and galactose, with only minor carbon source-dependent variations. In addition, one main polymeric population was identified that revealed a higher MW range when *B. adolescentis* was grown in the presence of GOS and GOS/2'-FL, compared to MRS4 medium containing glucose as sole carbon source.

In order to obtain more structural details of the polysaccharide's repeating unit, 1D- and 2D-NMR spectra were recorded. In Fig. 4, the stacked ^{1}H NMR spectra are presented of *B. adolescentis* EPS grown in the three different media. These spectra corroborate the expected similarity in the polysaccharide structures, based on the similar monosaccharide ratios, with the same peak pattern visible in the three samples.

Close examination of the 1D ^{1}H spectrum, supported with ^{13}C—^{1}H correlations from the 2D-HSQC spectra of the EPS sample isolated from GOS-supplemented medium indicated the presence of four anomeric signals in equal ratios at 5.55 ppm (α-Glc, residue **A**), 5.26 ppm (α-Gal, **B**), 4.77 ppm (β-Glc, **C**) and 4.64 ppm (β-Glc, **D**) (Fig. S1). The same anomeric signals were observed for the samples isolated from GOS/2'-FL and glucose media (Fig. 4). Using 2D COSY and TOCSY spectroscopy anomeric correlation tracks were developed fully for residues **A**, **C** and **D**, suggesting Glc-residues, while residue **B** developed up to H4 fitting a Gal residue (Table 3). 2D HSQC spectroscopy allowed correlation between established ^{1}H signals and ^{13}C signals for most residues (Table 3, Fig. S2). The ^{13}C chemical shifts for monosaccharide residues are well established and stable,(Bock & Pedersen, 1983; Bock & Thøgersen, 1983) and show a significant 5–10 ppm downfield shift upon substitution, and a 1–2 ppm upfield shift upon neighbouring substitution (Bock & Pedersen, 1983). Positions with clear downfield shifts of the ^{13}C chemical shift, indicative of a position with a glycosidic linkage, have been marked in boldface in Table 3. Correlations in a 2D ROESY spectrum were used to identify linkages between the residues, showing interactions between residue **A** H-1 and **B** H-1, clearly indicating a 2-substitution of either residue. The downfield shift of the **A** C-2 signal indicates a substitution of residue **A** by residue **B**. A downfield shift of the C-3 of residue **A** indicates a 3-substitution as well, but no residue could be assigned to link to this position. Residue **C** showed a downfield shift of the C-3 signal, and a ROESY correlation was established between residue **A** H-1 and residue **C** H-3. Residue **C** showed a ROESY correlation with residue **D** H-3, supported by a residue **D** C-3 downfield shift. Finally, residue **B** showed a 4-substitution evidenced by a C-4 downfield shift and a correlation between H-4 and **D** H-1 indicates a **D**1—4**B** element.

Interestingly, in the 2D HSQC spectrum two CH_2 signals at 3.51 and 3.66 ppm correlated with δ ^{13}C 63.6, which resemble CH_2OH signals observed with sialic acid-type monosaccharides. In addition, the CH_2 signals at 2.30 and 2.89 ppm correlate with δ^{13}C 44.0, which is indicative of the C-3 deoxy (CH_2) position in this type of carbohydrates (black circles, Fig. 5). Building up the TOCSY scalar network from the distinctive C-3 signals, combined with 2D HSQC correlations suggest at least a C-8 monosaccharide, although a C-9 2-keto-3-deoxy sugar cannot be excluded. To further prove the presence of a sialic acid-type monosaccharide, DMB labeling was performed on a hydrolyzed sample, (*B. adolescentis* GOS/2'-FL), and after analysis by UPLC-FLD, a major peak was observed, as well as two minor peaks (Fig. S3). The major peak showed the same retention time as Neu5Ac in the UPLC-FLD chromatogram, however the lack of a clear *N*-acetyl CH_3 peak in the 1D ^{1}H NMR spectrum indicates that the sialic acid type residue is not Neu5Ac. The major peak did not overlap with Neu5Gc, Kdo or Kdn, which were used as additional controls. These data suggest the possible presence of a novel 8- or 9-carbon 2-keto-3-deoxy-type sugar residue in this bacterial polysaccharide. Overall, from the NMR data a tentative structure of *B. adolescentis* EPS repeating unit was deduced to be [-3**D**1-4**B**1-2**A**1-3**C**1-], or in full nomenclature [→3)-β-Glc*p*-(1 → 4)-α-Gal*p*-(1 → 2)-α-Glc*p*-(1 → 3)-β-Glc*p*-(1→] (blue stars, Fig. 5).

In addition to this linear tetrasaccharide repeating unit, there is also evidence of extra branching positions that remain unidentified. The

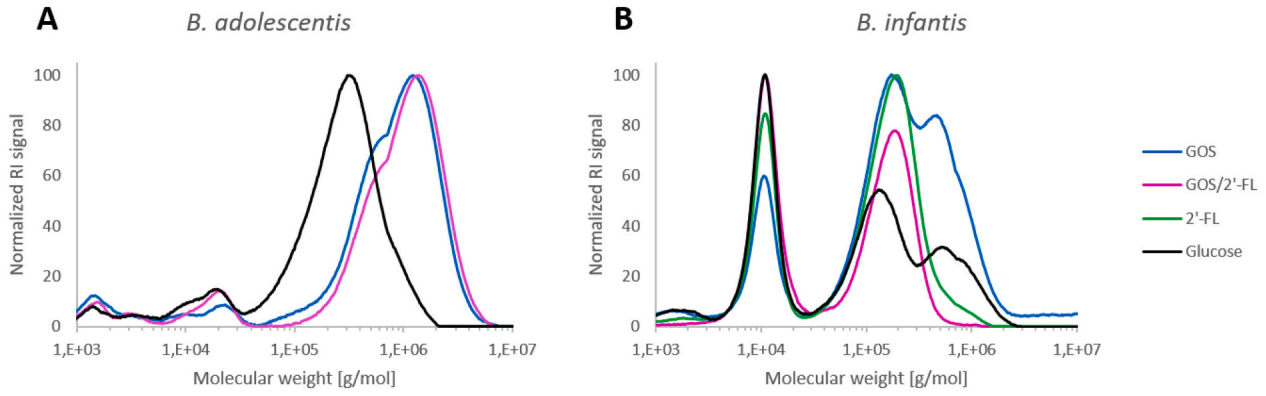

Fig. 3. GPC spectra for the molecular weight distribution of *B. adolescentis* (Panel A) and *B. infantis* (Panel B) EPS isolated from GOS (blue), GOS/2'-FL (pink), 2'-FL (green) and glucose (black). Only one of the analyzed replicates (n = 3) is reported in the figure.

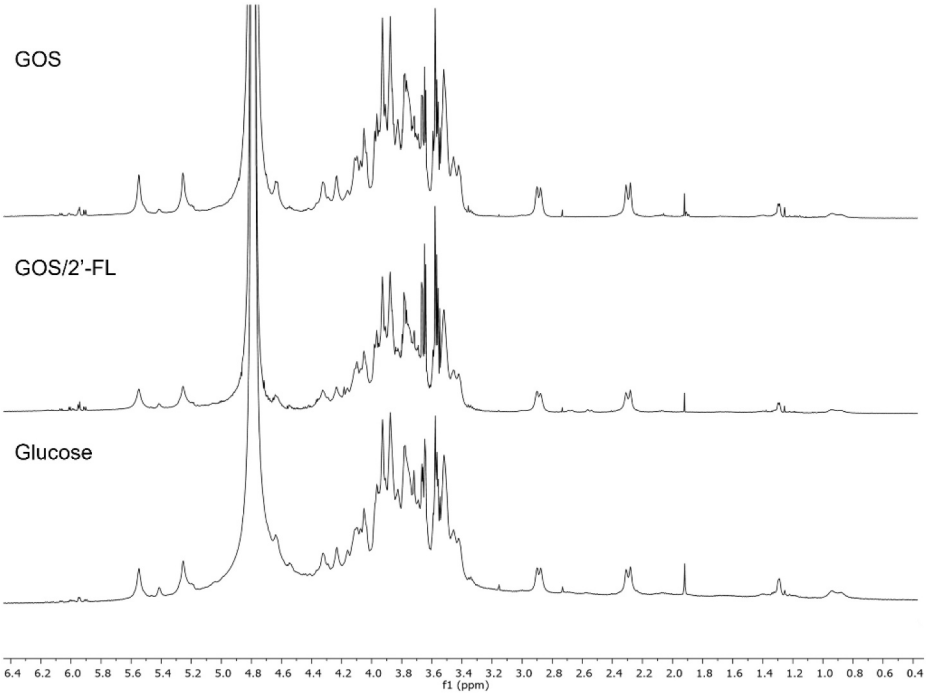

Fig. 4. Stacked ^{1}H NMR (600 MHz, D_2O) spectra of *B. adolescentis* EPS isolated from different carbon sources.

Table 3
^{1}H and ^{13}C chemical shifts of the residues belonging to the tetrasaccharide repeating unit of *B. adolescentis* EPS. Points of substitution, as evidenced by ^{13}C downfield shifts are marked in boldface. Chemical shift values are referenced to acetone as the internal standard.

		^{1}H and ^{13}C chemical shifts (ppm)						
		1	2	3	4	5	6a	6b
α-Glc*p* (A)	^{1}H	5.55	3.77	3.88	3.56	4.09	3.90	3.77
	^{13}C	96.1	**75.6**	**78.1**	69.2	71.4	60.3	60.3
α-Gal*p* (B)	^{1}H	5.26	3.93	4.03	4.22	4.16	4.07	3.77
	^{13}C	95.6	68.8	69.9	**79.0**	81.4	**65.3**	65.3
β-Glc*p* (C)	^{1}H	4.77	3.45	3.70	3.64	3.49	3.91	3.72
	^{13}C	102.6	75.3	**81.7**	70.1	75.5	60.3	60.3
β-Glc*p* (D)	^{1}H	4.64	3.51	3.76	3.45	3.50	3.77	3.81
	^{13}C	102.8	75.3	**84.4**	72.1	75.2	60.3	60.3

chemical shifts of the H-3/C-3 positions of unit **A** reveal a clear downfield shift (δ 3.88 and 78.1 ppm) that suggest another substitution at the C-3 position of the α-Glc*p* residue. On the α-Gal*p* (**B** unit), a 6-substitution is suggested by H6a and H6b signals at δ 4.07 and 3.77 ppm, correlating with a C-6 signal at 65.3 ppm, a clear downfield shift from 60 to 61 ppm where most unsubstituted C-6 signals reside. Since the Glc residues had fully developed anomeric tracks in the TOCSY spectrum, and showed no signal at 4.07 ppm, it is most likely a 6-substitution on the α-Gal*p* unit (residue **B**), where the TOCSY anomeric track does not develop beyond the H-4 signal. This is possibly where the sialic acid-type monosaccharide is linked. The amount of isolated EPS available for NMR analysis was insufficient for detailed 2D HMBC spectra, which could have identified the position of the sialic acid in the structure and support the tentative structure further. Future work should include isolation of sufficient EPS to perform partial acid hydrolysis studies as well as further detailed 2D NMR analysis.

In addition to the tentative repeating unit, an anomeric signal with lower intensity was detected at 5.40 ppm which is postulated to be an

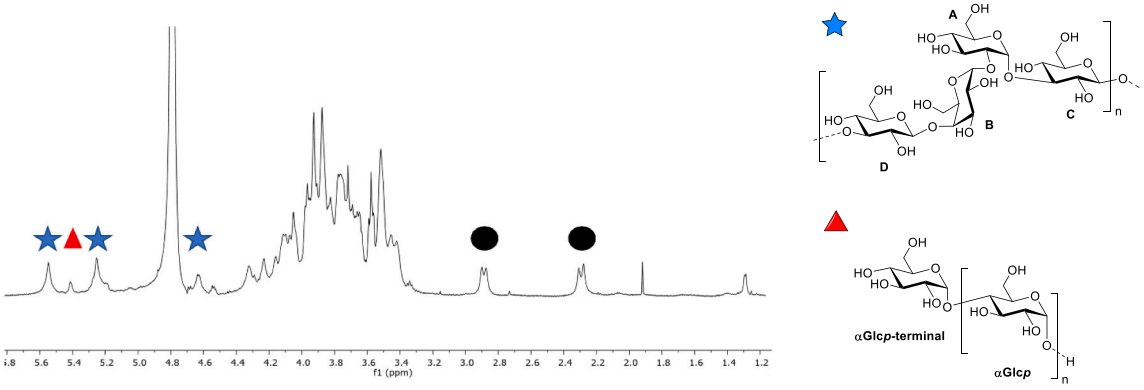

Fig. 5. ^{1}H NMR (600 MHz, D_2O) spectrum of the *B. adolescentis* EPS isolated from glucose-containing medium. Two main polysaccharides were identified: a tetrasaccharide repeating unit (anomeric signals marked by blue star) and an α-1,4-glucan (anomeric signal marked by red triangle). One of the anomeric signals belonging to the tetrasaccharide is masked by the D_2O peak. Black circles indicate the signals that were attributed to a sialic acid-type deoxysugar. Note that the absolute configuration (D/L) of the monosaccharides has not been determined.

α-1,4-glucan (see section 3.4.2), whose production seems increased in glucose-containing MRS4 medium (red triangle, Fig. 5).

3.4.2. EPS samples from B. infantis

The EPS samples isolated from *B. infantis* also contained glucose and galactose, similar to the EPS samples from *B. adolescentis*. However, in contrast to the *B. adolescentis* samples, the presence of 2'-FL and GOS/2'-FL in the growth media resulted in a marked decrease of the glucose/galactose ratio in the EPS samples, as compared to bacterial growth in the presence of GOS and glucose, which led to relatively more glucose in the EPS samples (Table 2).

The stacked ^{1}H NMR spectra of the EPS produced in the four carbon sources are shown in Fig. 6. From the ^{1}H NMR analysis, it is evident that the broad anomeric signal at 5.41 ppm was significantly more intense in the samples isolated from the medium containing GOS or glucose (MRS4 medium), compared to the samples isolated from 2'-FL- and GOS/2'-FL-containing media. When the anomeric signal at 5.41 ppm was analyzed by 2D ^{1}H—^{1}H TOCSY the spectrum showed four cross-peaks suggesting the presence of glucose (Gheysen et al., 2008). Furthermore a double pattern for the anomeric signal at 5.41 ppm was observed: one major peak pattern, fitting a 4-substituted α-Glc*p* residue and one minor peak pattern fitting a non-reducing terminal α-Glc*p* residue, as evidenced by the H-4 signal at δ 3.41 ppm (van Leeuwen et al., 2008).

The ROESY spectrum showed a unique correlation between the anomeric proton at 5.41 ppm and the proton at 3.65 ppm (H-4 of a nonterminal Glc residue), suggesting the presence of an [α-Glc*p*-(1,4)]$_n$ repeating unit (Table 4, red triangle in Fig. 7). Interestingly, this α-1,4-glucan structure, which was very apparent in EPS from the GOS- and glucose-containing medium, was only present in minor amounts in the samples isolated from 2'-FL and GOS/2'-FL medium, and was also detected in the *B. adolescentis* EPS samples (section 3.4.1).

A second polysaccharide was structurally characterized in the *B. infantis* samples as composed of the galactan disaccharide repeating unit [→3)-β-Gal*f*-(1 → 3)-α-Gal*p*-(1→] (blue diamonds, Fig. 7). The anomeric signal of the galactofuranoside was found at 5.20 ppm and a second anomeric signal from the galactopyranoside was detected at 5.07 ppm. Interestingly, the repeating unit was also present as a tetrasaccharide with both α-Gal*p* and β-Gal*f* units substituted on the 6 position (~80 % substitution calculated based on the ^{1}H signal intensity in the 1D ^{1}H NMR spectrum) with a terminal residue of β-1,6-linked glucopyranoside. The complete assignment of the polysaccharides is reported in Table 5 (^{13}C—^{1}H HSQC provided in Fig. S4). This assignment is in agreement with previous characterization of the EPS of *B. infantis* ATCC15697 (Tone-Shimokawa et al., 1996).

A third polysaccharide fraction composed of eight monosaccharide residues was identified in each of the EPS samples produced by *B. infantis*, but this was not fully characterized (black stars, Fig. 7). ^{1}H—^{1}H COSY, ^{13}C—^{1}H HSQC (Fig. S4) and TOCSY correlation spectra were used to assign ^{1}H chemical shifts starting from the 8 anomeric signals (Table 6). For residues **D**—**F**, **K** and **M** up to H-4 could be identified, which suggests these residues are galactose. Residues **G**, **H** and **L** correlated up to the H-6 signals, suggesting Glc residues. The H-1/C-1 chemical shifts of residue **D** (δ 5.44 and 108.0 ppm) fit with a Gal*f* residue, similar to the signals obtained with the galactan disaccharide (see above). However, in this case a slight downfield shift of the C-1 fits with a 2-substitution of this residue. Also, the H-2 correlated with a C-2

Table 4
^{1}H and ^{13}C chemical shifts of the residues belonging to the [α-Glc*p*-(1,4)]$_n$. Chemical shift values are referenced to acetone as the internal standard. Points of substitution, as evidenced by ^{13}C downfield shifts are marked in boldface.

		^{1}H and ^{13}C chemical shifts (ppm)						
		1	2	3	4	5	6a	6b
α-Glc*p*	^{1}H	5.40	3.65	3.98	3.65	3.85	3.85	3.81
	^{13}C	99.6	72.2	74.0	**78.4**	71.8	61.2	61.2
α-Glc*p* (terminal)	^{1}H	5.40	3.59	3.70	3.41	3.85	3.84	3.75
	^{13}C	99.6	72.5	73.6	70.3	73.1	61.2	61.2

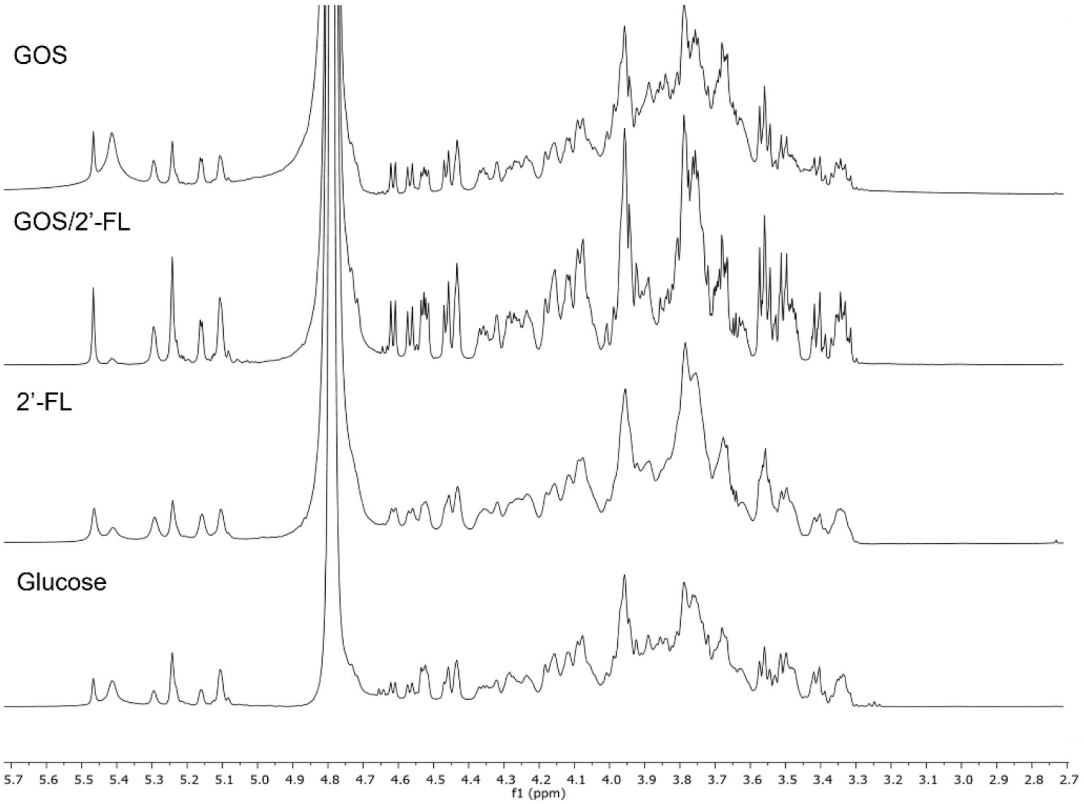

Fig. 6. Stacked ^{1}H NMR (600 MHz, D_2O) spectra of *B. infantis* EPS isolated from different carbon sources.

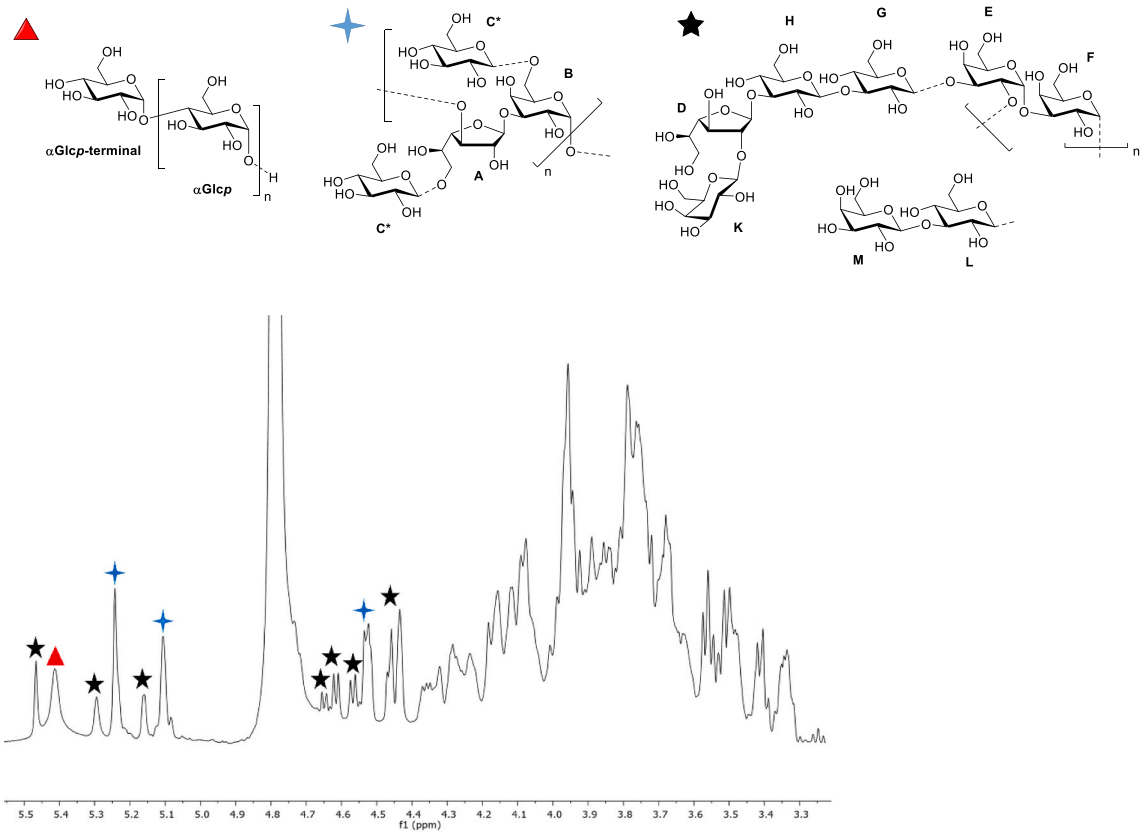

Fig. 7. ^{1}H NMR (600 MHz, D_2O) spectrum of *B. infantis* EPS isolated from glucose-containing medium. Three main polysaccharides were identified: an α-1,4-glucan (marked with a red triangle), a galactan (marked with a blue diamond) and an octasaccharide repeat (black star). Note that the absolute configuration (D/L) of the monosaccharides has not been determined.

Table 5
^{1}H and ^{13}C Chemical shifts of the residues belonging to the galactan polysaccharide. Residues marked with a * belong to the β-Glc*p* substituted galactan. Chemical shift values are referenced to acetone as the internal standard. Points of substitution, as evidenced by ^{13}C downfield shifts are marked in boldface.

		^{1}H and ^{13}C chemical shifts (ppm)						
		1	2	3	4	5	6a	6b
β-Gal*f* (A)	^{1}H	5.20	4.40	4.06	4.25	3.86	3.68	3.65
	^{13}C	109.2	79.8	84.4	81.8	70.8	62.6	62.6
α-Gal*p* (B)	^{1}H	5.07	3.93	4.13	3.94	4.13	3.74	3.74
	^{13}C	99.3	77.1	69.1	67.2	71.2	61.2	61.2
β-Gal*f* (A*)	^{1}H	5.20	4.40	4.06	4.25	4.07	4.05	3.78
	^{13}C	109.2	79.8	84.4	81.8	69.2	**71.1**	**71.1**
α-Gal*p* (B*)	^{1}H	5.07	3.93	4.13	3.94	4.33	3.86	3.86
	^{13}C	99.3	77.1	69.1	67.2	70.1	**69.6**	**69.6**
β-Glc*p* (C*)	^{1}H	4.50	3.31	3.51	3.38	3.45	3.71	3.91
	^{13}C	102.5	72.9	75.5	69.6	75.8	60.8	60.8

Table 6
^{1}H and ^{13}C Chemical shifts of the residues belonging to the putative octasaccharide repeat, identified using 1D and 2D NMR spectra in D_2O. Points of substitution, as evidenced by ^{13}C downfield shifts are marked in boldface. Chemical shift values are referenced to acetone as the internal standard.

	^{1}H and ^{13}C chemical shifts (ppm)						
	1	2	3	4	5	6a	6b
β-Gal*f* (D)	5.44	4.40	4.24	4.10			
	108.0	**88.5**	76.1	83.8			
α-Gal*p* (E)	5.27	4.15	4.21	4.30			
	95.0	**81.5**	**76.2**	69.3			
α-Gal*p* (F)	5.14	3.82	3.94	3.95			
	94.3	68.2	**77.5**	69.0			
β-Glc*p* (G)	4.72	3.54	3.73	3.52	3.47	3.88	3.75
	103.0	71.0	**85.8**	68.1	75.4	60.5	60.5
β-Glc*p* (H)	4.70	3.71	3.78	3.60	3.68	3.87	3.81
	103.0	70.6	**80.2**	74.3	75.2	60.5	60.5
β-Gal*p* (K)	4.57	3.54	3.67	3.93			
	101.9	74.2	74.6	69.1			
β-Glc*p* (L)	4.54	3.33	3.66	3.60	3.48	3.97	3.88
	102.3	73.1	**78.4**	74.6	75.3	60.2	60.2
β-Gal*p* (M)	4.44	3.54	3.67	3.91			
	103.3	70.7	74.6	68.9			

at 88.5 ppm, a clear downfield shift compared with residue **A** in the galactan disaccharide, indicating 2-substitution of Gal*f* residue **D**. The ROESY spectrum shows a correlation between **K** H-1 and **D** H-1 and H-2. Moreover, there is a correlation in the 2D HMBC spectrum between **K** H-1 and **D** C-2, indicating a **K**1—2**D** element. Residue **K** shows a pattern of a β-Gal residue that is not substituted on the 2, 3, or 4 position, and a 6-substitution cannot be excluded for this residue. Residue **H** shows a pattern of a 3-substituted β-Glc residue, evidenced by a downfield shift of C-3 to δ 80.2 ppm. The 2D ROESY spectrum shows a correlation between **D** H-1 and **H** H-3, also supported by HMBC correlations, leading to a **D**1—3**H** element. Residue **G** showed also a pattern fitting a 3-substituted β-Glc residue. ROESY and HMBC correlations support a **H**1-3**G** element. Together these data show a potential **K**1-2**D**1-3**H**1-3**G** structural element; i.e. β-Gal*p*-(1 → 2)-β-Gal*f*-(1 → 3)-β-Glc*p*-(1 → 3)-β-Glc*p*.

Residue **E** shows a pattern up to H-4 fitting a 2,3-disubstituted α-Gal*p* residue, with chemical shifts of H-2/C-2 at δ 4.15/81.5 ppm and H-3/C-3 at δ 4.21/76.2 ppm. There are ROESY correlations between **E** H-1 and **F** H-1, as well as between **F** H-1 and **E** H-2, indicating an **F**1-2**E** element; however, the HMBC spectrum showed no correlations for **F** and **E** residues. Residue **F** shows a 3-substitution, with a downfield shift of C-3.

The ROESY spectrum shows a correlation between **E** H-1 and **F** H-3, suggesting a [-3**F**1-2**E**1-] repeating unit as the backbone of this polysaccharide. In addition, there is an extensive branch on the **E** 3-position. Correlations between **G** H-1 and **E** H-3 in the ROESY spectrum suggest that the tentative structure **K**1-2**D**1-3**H**1-3**G** is attached to the 3-position of residue **E**. This branching tetrasaccharide seems to be present on almost each **E** residue, as the integrals for the signals nicely align with each other in equal ratios.

Lastly, there is a disaccharide element containing Glc*p* residue **L** with a 3-substitution as shown by a C-3 downfield shift. Residue **M** shows the pattern of a terminal β-Gal*p* residue. Correlations in the ROESY spectrum between **M** H-1 and **L** H-3, as well as HMBC correlations supporting this linkage, indicate an **M**1-3**L** element. The HMBC spectrum also shows a correlation between **L** H-1 and a carbon signal at δ 68.5 ppm, fitting a 1,6-linkage. This indicates an **M**1-3**L**1–6 disaccharide branch. Because TOCSY correlations reveal that these substituted H6 signals do not belong to a Glc residue, it is suggested that one of the Gal residues is branched on C-6. From the available data it is not possible to exactly identify the branched Gal unit.

In summary, β-Gal*f*, β-Gal*p*, β-Glc*p* and α-Gal*p* residues were identified in the octasaccharide but it was not possible to fully identify the connection and substitution pattern. Future analysis by partial acid hydrolysis and linkage analysis by partially methylated alditol acetates could help further elucidate this structure.

The results obtained from the NMR structural analysis of *B. infantis* EPS corroborated the difference in galactose/glucose ratios obtained from the EPS isolated from different carbon sources. It was shown that *B. infantis* EPS isolates obtained from GOS- and glucose-containing media were characterized by a higher amount of an amylose-like polysaccharide (α-1,4-glucan) while 2'-FL and GOS/2'-FL samples were mainly containing the galactan fraction (blue diamonds, Fig. 7) and the unidentified octasaccharide repeat (black stars Fig. 7). By comparing the integration of the anomeric peaks belonging to the octasaccharide repeat and to the galactan (approximately 1/1 for GOS and 2'-FL, and 1/2 for GOS/2'-FL and glucose), glucose and GOS/2'-FL seem to better stimulate the formation of the galactan which is less abundant in the samples isolated from *B. infantis* with only 2'-FL or GOS. Furthermore, the GPC analysis already indicated the presence of different polysaccharidic fractions in the samples, which is now confirmed by the NMR data which showed the presence of three main polysaccharides. This also suggests that the highest MW population (300–700 kDa) corresponds to the α-1,4-glucan (Fig. 3).

4. Discussion and concluding remarks

Beneficial commensal bacteria, unlike pathogenic bacteria, can ferment specific classes of non-digestible carbohydrates, especially HMOs, which give them a growth benefit. Bifidobacteria can metabolize HMOs using different mechanisms, which vary across different species (Sela & Mills, 2010). For instance, *B. infantis* is able to import intact HMO structures followed by the intracellular fermentation into monosaccharide components with a dedicated gene cluster for HMO-digestion has been identified (Sela et al., 2008). However, HMO digestion is limited to a selection of bifidobacteria strains, as several strains are unable to grow on HMOs, including *B. adolescentis* (Ward et al., 2007). Interestingly, a wider variety of bacterial species is able to grow on GOS, as is clear from their increase in bacterial numbers when GOS are supplemented (Matsuki et al., 2016; Salli et al., 2021). These facts are in agreement with our observations that both *B. adolescentis* and *B. infantis* grow equally well in GOS-supplemented media, while *B. adolescentis* is unable to grow with 2'-FL supplementation alone.

Intestinal *B. infantis* colonization and growth is a major target of the supplementation of infant formula with molecules such as 2'-FL and GOS. Supporting *B. infantis* growth in early life is associated with many health benefits including lowering chances on atopic allergies and metabolic issues (Oerlemans et al., 2021). Recently, we and others have suggested that EPS from beneficial bacteria might be responsible for these health effects (R. Akkerman et al., 2024; Fernández-Lainez et al., 2022). Here we show that 2'-FL and GOS not only facilitate the growth of *B. infantis* but have also an effect on the structural characteristics of its EPS. What this means for the efficacy of conveying health benefits remains to be demonstrated but it seems that the impact of 2'-FL and GOS goes beyond increasing numbers and also changes behaviour of these beneficial bacteria.

To explain the impact of different carbon sources on the changes in EPS production observed in this project, a thorough understanding of the genes responsible for EPS biosynthesis is required. With the rise of genome sequencing, more information is available on the genes and gene clusters that are responsible for EPS biosynthesis. However, in contrast to the gene clusters from lactic acid bacteria (LAB), which share a consensus organization, the EPS genes in bifidobacteria are less organized (Hidalgo-Cantabrana et al., 2014). One gene that shares high homology between bifidobacterial species is the priming glycosyltransferase (pGT), which performs the first transfer to start the EPS repeat synthesis (Hidalgo-Cantabrana et al., 2014). To the best of our knowledge, the only EPS biosynthesis cluster that has been characterized is from *B. longum* subsp. *longum* 35624™ (Altmann et al., 2016). Next to the pGT, the EPS-cluster includes genes for general GTs, polymerization and export. In the case of *B. adolescentis,* since the major impact of GOS and GOS/2'-FL was on the size distribution of the EPS, it would be very interesting to understand if gene levels of the proteins involved in polymerization and chain-length determination are impacted. For *B. infantis* especially a change in levels of the α-1,4-glucan were observed, suggesting that the genes for α-1,4-glucan production may change in the presence of different carbon sources. Annotating the EPS biosynthesis genes in *B. adolescentis* DSM20083 and *B. infantis* DSM20088 will be essential to start linking gene transcription levels to specific growth conditions, which is an important step towards explaining the effect of the carbon source on EPS composition.

Finally, we report novel structures for the EPS repeats of both *B. adolescentis* and *B. infantis*. An increasing number of bifidobacterial EPS structures are becoming available, and our findings are in line with the high abundance of Glc*p* and Gal*p* residues in the backbone and as branching residues as observed in other bifidobacteria (Kohno et al., 2009; Sadeghi et al., 2024). Moreover, larger repeating units, consisting of five to seven monosaccharides, are also reported (Sadeghi et al., 2024). However, the finding that the bifidobacteria studied here produce high molecular weight α-1,4-glucan polysaccharides was unexpected. α-Glucans comprise a large family of differently linked α-glucan polysaccharides, including amylose, reuteran, and dextrans. Generally, these homopolysaccharides are synthesized extracellularly by glucansucrase enzymes, and this synthesis has been mostly observed by LAB, such as Lactobaccilli. In contrast, the production of α-glucans by bifidobacteria has not been reported, whereas several probiotic strains are able to degrade α-1,4-glucans (Møller et al., 2014). In an attempt to explain the production of α-1,4-glucan repeats, the published genomes of *B. adolescentis* (ATCC 15703, NC_008618.1) and *B. infantis* (ATCC 15697, NC_011593.1) (Sela et al., 2008) were mined for any gene that could be involved in α-glucan processing. By using the annotation from NCBI from homology of characterized genes and proteins, four genes were identified that may be involved in α-1,4-glucan assembly: *glgE* (α-1,4-glucan:maltose-1-phosphate maltosyltransferase), *glgB* (1,4-α-glucan branching enzyme), *malQ* (4-α-glucanotransferase) (Jeong et al., 2019), and *gtfA* (1,4-α-oligoglucan phosphorylase). As it is known that the addition of different carbohydrate carbon sources can differently stimulate expression of genes involved in EPS biosynthesis, (Yu Zhang et al., 2021) future studies on gene expression levels of these genes in response to growth with different carbon sources may reveal any link that may exist between them.

In summary, in this study the impact of 2'-FL, GOS and GOS/2'-FL on the growth, EPS production and structural identity from *B. infantis* (DSM 20088) and *B. adolescentis* (DSM20083) was investigated. While 2'-FL

did not support growth of *B. adolescentis*, the other carbon sources resulted in larger polymeric populations of EPS from *B. adolescentis*. Interestingly, all carbon sources supported the growth of *B. infantis*, with 2'-FL as carbon source resulting in increased growth rates. The EPS isolated from *B. infantis* grown with 2'-FL and GOS/2'-FL revealed a relatively reduced glucose content. The NMR structural characterization clarified that the production of α-1,4-glucan by *B. infantis* is highly reduced when 2'-FL and GOS/2'-FL are used as carbon sources. These findings show that different carbon sources have a significant impact on the resulting EPS structures.

Further investigations are necessary to assess if the structural diversity can impact the biological activity of the EPS isolates. Furthermore, a more detailed structural characterization for the octasaccharide repeating unit of the EPS produced by *B. infantis* is needed. For this goal, the fractionation of the EPS mixture by size exclusion chromatography would ease the structural characterization efforts. Finally, evaluating gene expression in *B. infantis* and *B. adolescentis,* in presence of different carbon sources, may afford a rationale to understand how different carbohydrates influence EPS production and composition.

CRediT authorship contribution statement

Michela Ferrari: Writing – review & editing, Writing – original draft, Methodology, Investigation, Conceptualization. **Sander S. van Leeuwen:** Writing – review & editing, Writing – original draft, Methodology, Investigation. **Paul de Vos:** Writing – review & editing, Conceptualization. **Edita Jurak:** Writing – review & editing, Writing – original draft, Supervision, Methodology, Investigation. **Marthe T.C. Walvoort:** Writing – review & editing, Writing – original draft, Supervision, Funding acquisition, Conceptualization.

Declaration of competing interest

The authors declare that they have no known competing financial interests or personal relationships that could have appeared to influence the work reported in this paper.

Data availability

Data will be made available on request.

Acknowledgements

We thank Lisanne Hameleers for her assistance in performing the HPAEC measurements. This work was financially supported by a NWO-CCC 'CarboBiotics' grant (ALWCC.2017.005), which is from a public-private partnership between the Dutch Organization for Scientific Research, FrieslandCampina, NuScience and Avebe, coordinated by the Carbohydrate Competence Center (www.cccresearch.nl).

Appendix A. Supplementary data

Supplementary data to this article can be found online at https://doi.org/10.1016/j.carbpol.2024.122660.

References

Abdalla, A. K., Ayyash, M. M., Olaimat, A. N., Osaili, T. M., Al-Nabulsi, A. A., Shah, N. P., & Holley, R. (2021). Exopolysaccharides as antimicrobial agents: Mechanism and Spectrum of activity. *Frontiers in Microbiology, 12*, Article 664395.

Akkerman, R., Logtenberg, M. J., Beukema, M., de Haan, B. J., Faas, M. M., Zoetendal, E. G., … de Vos, P. (2022). Combining galacto-oligosaccharides and 2′-fucosyllactose alters their fermentation kinetics by infant fecal microbiota and influences AhR-receptor dependent cytokine responses in immature dendritic cells. *Food & Function, 13*, 6510–6521.

Akkerman, R., Oerlemans, M. M. P., Ferrari, M., Fernández-Lainez, C., de Haan, B. J., Faas, M. M., & de Vos, P. (2024). Exopolysaccharide β-(2,6)-Levan-type fructans have a molecular-weight-dependent modulatory effect on toll-like receptor signalling. *Food & Function, 15*(2), 676–688.

Altmann, F., Kosma, P., O'Callaghan, A., Leahy, S., Bottacini, F., Molloy, E., & O'Mahony, L. (2016). Genome analysis and characterisation of the exopolysaccharide produced by *Bifidobacterium longum* subsp. *longum* 35624™. *PLoS One, 11*(9), Article e0162983.

Bock, K., & Pedersen, C. (1983). Carbon-13 nuclear magnetic resonance spectroscopy of monosaccharides. In R. S. Tipson, & D. Horton (Eds.), *Advances in carbohydrate chemistry and biochemistry* (pp. 27–66). Academic Press.

Bock, K., & Thøgersen, H. (1983). Nuclear magnetic resonance spectroscopy in the study of mono- and oligosaccharides. In G. A. Webb (Ed.), *Annual reports on NMR spectroscopy* (pp. 1–57). Academic Press.

Bode, L. (2012). Human milk oligosaccharides: Every baby needs a sugar mama. *Glycobiology, 22*, 1147–1162.

Bunesova, V., Lacroix, C., & Schwab, C. (2016). Fucosyllactose and L-fucose utilization of infant *Bifidobacterium longum* and *Bifidobacterium kashiwanohense*. *BMC Microbiology, 16*(1).

Cheng, L., Akkerman, R., Kong, C., Walvoort, M. T. C., & de Vos, P. (2021). More than sugar in the milk: Human milk oligosaccharides as essential bioactive molecules in breast milk and current insight in beneficial effects. *Critical Reviews in Food Science and Nutrition, 61*, 1184–1200.

De Vuyst, L., & Degeest, B. (1999). Heteropolysaccharides from lactic acid bacteria. *FEMS Microbiology Reviews, 23*(2), 153–177.

Fernández-Lainez, C., Akkerman, R., Oerlemans, M. M. P., Logtenberg, M. J., Schols, H. A., Silva-Lagos, L. A., & de Vos, P. (2022). β(2→6)-type fructans attenuate proinflammatory responses in a structure dependent fashion via toll-like receptors. *Carbohydrate Polymers, 277*, Article 118893.

Ferrari, M., Hameleers, L., Stuart, M. C. A., Oerlemans, M. M. P., de Vos, P., Jurak, E., & Walvoort, M. T. C. (2022). Efficient isolation of membrane-associated exopolysaccharides of four commercial bifidobacterial strains. *Carbohydrate Polymers, 278*, Article 118913.

Garrido, D., Dallas, D. C., & Mills, D. A. (2013). Consumption of human milk glycoconjugates by infant-associated bifidobacteria: Mechanisms and implications. *Microbiology-Sgm, 159*, 649–664.

Gheysen, K., Mihai, C., Conrath, K., & Martins, J. C. (2008). Rapid identification of common Hexapyranose monosaccharide units by a simple TOCSY matching approach. *Chemistry - A European Journal, 14*, 8869–8878.

Grobben, G. J., Sikkema, J., Smith, M. R., & Debont, J. A. M. (1995). Production of extracellular polysaccharides by *Lactobacillus delbrueckii* ssp *bulgaricus* NCFB 2772 grown in a chemically-defined medium. *Journal of Applied Bacteriology, 79*(1), 103–107.

Harazono, A., Kobayashi, T., Kawasaki, N., Itoh, S., Tada, M., Hashii, N., & Yamaguchi, T. (2011). A comparative study of monosaccharide composition analysis as a carbohydrate test for biopharmaceuticals. *Biologicals, 39*, 171–180.

Hidalgo-Cantabrana, C., Sanchez, B., Milani, C., Ventura, M., Margolles, A., & Ruas-Madiedo, P. (2014). Genomic overview and biological functions of exopolysaccharide biosynthesis in Bifidobacterium spp. *Applied and Environmental Microbiology, 80*(1), 9–18.

Ibarburu, I., Soria-Díaz, M. E., Rodríguez-Carvajal, M. A., Velasco, S. E., Tejero-Mateo, P., Gil-Serrano, A. M., Irastorza, A., & Dueñas, M. T. (2007). Growth and exopolysaccharide (EPS) production by Oenococcus oeni I4 and structural characterization of their EPSs. *Journal of Applied Microbiology, 103*, 477–486.

Jeong, D. W., Jeong, H. M., Shin, Y. J., Woo, S. H., & Shim, J. H. (2019). Properties of recombinant 4-α-glucanotransferase from Bifidobacterium longum subsp. longum JCM 1217 and its application. *Food Science and Biotechnology, 29*, 667–674.

Jurak, E., Kabel, M. A., & Gruppen, H. (2014). Carbohydrate composition of compost during composting and mycelium growth of *Agaricus bisporus*. *Carbohydrate Polymers, 101*, 281–288.

Kohno, M., Suzuki, S., Kanaya, T., Yoshino, T., Matsuura, Y., Asada, M., & Kitamura, S. (2009). Structural characterization of the extracellular polysaccharide produced by Bifidobacterium longum JBL05. *Carbohydrate Polymers, 77*(2), 351–357.

Kong, C., Faas, M. M., de Vos, P., & Akkerman, R. (2020). Impact of dietary fibers in infant formulas on gut microbiota and the intestinal immune barrier. *Food & Function, 11*, 9445–9467.

Looijesteijn, P. J., Trapet, L., de Vries, E., Abee, T., & Hugenholtz, J. (2001). Physiological function of exopolysaccharides produced by *Lactococcus lactis*. *International Journal of Food Science, 64*, 71–80.

Macy, J. M., Snellen, J. E., & Hungate, R. E. (1972). Use of syringe methods for anaerobiosis. *American Journal of Clinical Nutrition, 25*(12), 1318–1323.

Martins, G. N., Ureta, M. M., Tymczyszyn, E. E., Castilho, P. C., & Gomez-Zavaglia, A. (2019). Technological aspects of the production of Fructo and Galacto-oligosaccharides. Enzymatic synthesis and hydrolysis. *Frontiers. Nutrition, 6*.

Matsuki, T., Tajima, S., Hara, T., Yahagi, K., Ogawa, E., & Kodama, H. (2016). Infant formula with galacto-oligosaccharides (OM55N) stimulates the growth of indigenous bifidobacteria in healthy term infants. *Beneficial Microbes, 7*, 453–461.

Møller, M., Goh, Y., Viborg, A., Andersen, J., Klaenhammer, T., Svensson, B., & Hachem, M. A. (2014). Recent insight in α-glucan metabolism in probiotic bacteria. *Biologia, 69*, 713–721.

Oerlemans, M. M. P., Akkerman, R., Ferrari, M., Walvoort, M. T. C., & de Vos, P. (2021). Benefits of bacteria-derived exopolysaccharides on gastrointestinal microbiota, immunity and health. *Journal of Functional Foods, 76*, Article 104289.

Ojima, M. N., Asao, Y., Nakajima, A., Katoh, T., Kitaoka, M., Gotoh, A., & Hirose, J. (2022). Diversification of a Fucosyllactose transporter within the genus Bifidobacterium. *Environmental Microbiology, 88*(2), Article e0143721.

Petry, S., Furlan, S., Crepeau, M. J., Cerning, J., & Desmazeaud, M. (2000). Factors affecting exocellular polysaccharide production by Lactobacillus delbrueckii subsp.

bulgaricus grown in a chemically defined medium. *Applied and Environmental Microbiology, 66*, 3427–3431.
Polak-Berecka, M., Wasko, A., Szwajgier, D., & Choma, A. (2013). Bifidogenic and antioxidant activity of exopolysaccharides produced by Lactobacillus rhamnosus E/N cultivated on different carbon sources. *Polish Journal of Microbiology, 62*, 181–189.
Pyclik, M., Srutkova, D., Schwarzer, M., & Gorska, S. (2020). Bifidobacteria cell wall-derived exo-polysaccharides, lipoteichoic acids, peptidoglycans, polar lipids and proteins - their chemical structure and biological attributes. *International Journal of Biological Macromolecules, 147*, 333–349.
Sadeghi, M., Haghshenas, B., & Nami, Y. (2024). Bifidobacterium exopolysaccharides: New insights into engineering strategies, physicochemical functions, and immunomodulatory effects on host health. *Frontiers in Microbiology, 15*.
Salli, K., Hirvonen, J., Siitonen, J., Ahonen, I., Anglenius, H., & Maukonen, J. (2021). Selective utilization of the human Milk oligosaccharides 2′-Fucosyllactose, 3-Fucosyllactose, and Difucosyllactose by various probiotic and pathogenic Bacteria. *Journal of Agricultural and Food Chemistry, 69*, 170–182.
Sela, D. A., Chapman, J., Adeuya, A., Kim, J. H., Chen, F., Whitehead, T. R., & Mills, D. A. (2008). The genome sequence of Bifidobacterium longum subsp infantis reveals adaptations for milk utilization within the infant microbiome. *Proceedings of the National Academy of Sciences of the United States of America, 105*(48), 18964–18969.
Sela, D. A., & Mills, D. A. (2010). Nursing our microbiota: Molecular linkages between bifidobacteria and milk oligosaccharides. *Trends in Microbiology, 18*(7), 298–307.
Shi, Y., Yokoyama, T., Akiyama, T., Yashiro, M., & Matsumoto, Y. (2012). Degradation kinetics of monosaccharides in hydrochloric, sulfuric, and sulfurous acid. *BIORESOURCES, 7*, 4085–4097.
Teixeira, P. (2014). LACTOBACILLUS | *Lactobacillus delbrueckii* ssp. *bulgaricus*. *Encyclopedia of Food Microbiology*.
Tone-Shimokawa, Y., Toida, T., & Kawashima, T. (1996). Isolation and structural analysis of polysaccharide containing galactofuranose from the cell walls of Bifidobacterium infantis. *Journal of Bacteriology, 178*(1), 317–320.
Torino, M. I., Font de Valdez, G., & Mozzi, F. (2015). Biopolymers from lactic acid bacteria. Novel applications in foods and beverages. *Frontiers in Microbiology, 6*, 834.
van Leeuwen, S. S., Leeflang, B. R., Gerwig, G. J., & Kamerling, J. P. (2008). Development of a 1H NMR structural-reporter-group concept for the primary structural characterisation of α-d-glucans. *Carbohydrate Research, 343*, 1114–1119.
Vandenplas, Y., Berger, B., Carnielli, V. P., Ksiazyk, J., Lagstrom, H., Luna, M. S., & Wabitsch, M. (2018). Human Milk oligosaccharides: 2-Fucosyllactose (2-FL) and lacto-N-Neotetraose (LNnT) in infant formula. *Nutrients, 10*(9), 1161.
Ward, R. E., Niñonuevo, M., Mills, D. A., Lebrilla, C. B., & German, J. B. (2007). In vitro fermentability of human milk oligosaccharides by several strains of bifidobacteria. *Molecular Nutrition & Food Research, 51*, 1398–1405.
Yang, S., Xu, X. Q., Peng, Q., Ma, L., Qiao, Y., & Shi, B. (2023). Exopolysaccharides from lactic acid bacteria, as an alternative to antibiotics, on regulation of intestinal health and the immune system. *Animal Nutrition, 13*, 78–89.
Yu Zhang, Y., Dai, X., Jin, H., Man, C., & Jiang, Y. (2021). The effect of optimized carbon source on the synthesis and composition of exopolysaccharides produced by Lactobacillus paracasei. *Journal of Dairy Science, 104*, 4023–4032.
Zabel, B., Yde, C. C., Roos, P., Marcussen, J., Jensen, H. M., Salli, K., & Morovic, W. (2019). Novel genes and metabolite trends in Bifidobacterium longum subsp. infantis bi-26 metabolism of human Milk oligosaccharide 2′-fucosyllactose. *Scientific Reports, 9*, 7983.
Zeuner, B., Teze, D., Muschiol, J., & Meyer, A. S. (2019). Synthesis of human milk oligosaccharides: Protein engineering strategies for improved enzymatic transglycosylation. *Molecules, 24*(11), 2033.